DeltaNp73 regulates neuronal survival in vivo

Fadel Tissir[a,1], Aurélia Ravni[a], Younès Achouri[a,2], Dieter Riethmacher[b], Gundela Meyer[c], and Andre M. Goffinet[a,1]

[a]Université catholique de Louvain, Institute of Neuroscience, Developmental Neurobiology Unit, B1200 Brussels, Belgium; [b]Southampton University School of Medicine, Southampton, United Kingdom; and [c]Facultad de Medicina, Universidad de La Laguna, Tenerife, Spain

Edited by Pasko Rakic, Yale University School of Medicine, New Haven, CT, and approved August 4, 2009 (received for review March 25, 2009)

Apoptosis occurs widely during brain development, and p73 transcription factors are thought to play essential roles in this process. The p73 transcription factors are present in two forms, the full length TAp73 and the N-terminally truncated DeltaNp73. In cultured sympathetic neurons, overexpression of DeltaNp73 inhibits apoptosis induced by nerve growth factor withdrawal or p53 overexpression. To probe the function of DeltaNp73 in vivo, we generated a null allele and inserted sequences encoding the recombinase Cre and green fluorescent protein (EGFP). We show that *DeltaNp73* is heavily expressed in the thalamic eminence (TE) that contributes neurons to ventral forebrain, in vomeronasal neurons, Cajal-Retzius cells (CRc), and choroid plexuses. In *DeltaNp73*$^{-/-}$ mice, cells in preoptic areas, vomeronasal neurons, GnRH-positive cells, and CRc were severely reduced in number, and choroid plexuses were atrophic. This phenotype was enhanced when DeltaNp73–positive cells were ablated by diphtheria toxin expression. However, ablation of cells that express DeltaNp73 and Wnt3a did neither remove all CRc, nor did they abolish Reelin secretion or generate a *reeler*-like cortical phenotype. Our data emphasize the role of DeltaNp73 in neuronal survival in vivo and in choroid plexus development, the importance of the TE as a source of neurons in ventral forebrain, and the multiple origins of CRc, with redundant production of Reelin.

Cajal-Retzius cells | p73 | Reelin | thalamic eminence | vomeronasal nerve

The *p73* locus (1) codes for transcription factors with close similarity to p53 and p63, two proteins implicated in tumor growth and in development (2– 4). During embryogenesis, *p73* is heavily expressed in restricted brain cell populations that include Cajal-Retzius cells in the embryonic telencephalic marginal zone (CRc), neurons in the vomeronasal organ (VNO) and preoptic areas, and choroid plexuses. (Note: CRc are a heterogenous cell population, and their molecular definition is controversial. For sake of simplicity, here we define them operationally as "transient Reelin-positive horizontal neurons in the embryonic telencephalic marginal zone," thus considering Reelin expression as their main molecular signature.)

Several mRNA and proteins are generated from the *p73* locus, through use of two promoters and several alternative polyadenylation sites. A first group of transcripts, named TAp73, are produced from promoter 1 upstream of exon 1, and encode proteins that are activated following DNA damage and promote cell death (5). A second set of transcripts are initiated from an alternative promoter in the third intron (promoter 2). They encode DeltaNp73 proteins that lack the N-terminal transactivation domain and are devoid of direct transcriptional activity. However, these shortened proteins are able to bind to DNA and to form dimers with TAp73, as well as with p53 and p63, thereby behaving as dominant negative, cell survival factors (6–11).

Inactivation of all p73 isoforms in mice is compatible with grossly normal development and survival, even though a large majority of *p73*$^{-/-}$ animals develop poorly, are runts, and die during their second or third postnatal week. In *p73*$^{-/-}$ mice, the number of CRc is dramatically reduced, the shape of the dentate gyrus is abnormal, with amputation of the lower blade, and the hippocampal fissure fails to form (2, 12). Intriguingly, the near absence of CRc, which is predicted to decrease Reelin secretion drastically, does not lead to a malformation of the cortical plate typical of Reelin-deficient (*reeler*) mice (2). Selective inactivation of *TAp73* isoforms leads to sterility, increased susceptibility to spontaneous and induced neoplasia, and subtle abnormalities of the granule cell layer in the dentate gyrus, but it does not affect development of CRc (13, 14).

To study the function of DeltaNp73 in vivo, we inactivated it specifically in mice, while inserting in the locus sequences that encode the recombinase Cre and the enhanced green fluorescent protein (EGFP). Using that new allele, we refine the expression canvas and demonstrate the role of DeltaNp73 in cell survival in vivo. Our data emphasize the importance of the thalamic eminence (TE) as a largely unsuspected source of neurons destined for ventral forebrain, as well as the multiple origins of CRc and their redundant production of Reelin.

Results

Production and Validation of *DeltaNp73* Mutant Mice. *DeltaNp73* transcripts are produced from promoter 2 in the third intron of the *p73* gene, and translation is initiated at an AUG in exon 3′, followed by splicing to exon 4. To target *DeltaNp73* whilst leaving the TAp73 isoforms unaffected, homology arms corresponding to sequences in intron 3 that flank exon 3′ were isolated from PAC clone RPCI-21 205D9 (RZPD, Germany). A sequence encoding the Cre recombinase was inserted in phase with the reading frame of the DeltaNp73 protein, using the methionine encoded by the endogenous AUG codon. The Cre sequence was followed by an internal ribosome entry site (IRES) and then by a sequence encoding the EGFP protein (Fig. 1*A*). Heterozygous and homozygous *DeltaNp73* mutant mice looked healthy and survived. However, homozygous mutants of both sexes had impaired fertility, particularly evident for females that generated only two or three litters. Using reverse transcription–polymerase chain reaction (RT-PCR), we showed that the *DeltaNp73* mRNA was absent in brain extracts from newborn *DeltaNp73* mutant mice, whereas *TAp73* transcripts were unaffected, confirming the selective inactivation of the DeltaNp73 forms (Fig. 1*B*). When *DeltaNp73* mice were crossed with ROSA26R reporter mice, we observed blue CRc in the marginal zone of the embryonic hemispheres, showing that the Cre sequence knocked in the locus was functional (Fig. 1*C* and Fig. 2 *B* and *F*). We also detected spontaneously fluorescent CRc in vibratome sections, demonstrating endogenous expression of EGFP from the knocked-in gene (Fig. 1*D*). Cre activity in the targeted locus was further demonstrated in crosses with mice that express DTA conditionally (15), which resulted in the ablation of all fluorescent cells (Fig. 1*E*).

Multiple Populations of DeltaNp73-Positive Cells in the Forebrain. We studied expression of DeltaNp73 in heterozygous mice from E11.5 to adult, by observing the fluorescence related to EGFP expression,

Author contributions: F.T. and A.M.G. designed research; F.T. and A.R. performed research; Y.A. and D.R. contributed new reagents/analytic tools; F.T. analyzed data; and F.T., G.M., and A.M.G. wrote the paper.

The authors declare no conflict of interest.

This article is a PNAS Direct Submission.

[1]To whom correspondence may be addressed. E-mail: fadel.tissir@uclouvain.be or andre.goffinet@uclouvain.be.

[2]Present address: Université catholique de Louvain, Plateforme de transgenèse, B1200 Brussels, Belgium.

This article contains supporting information online at www.pnas.org/cgi/content/full/0903191106/DCSupplemental.

NEUROSCIENCE

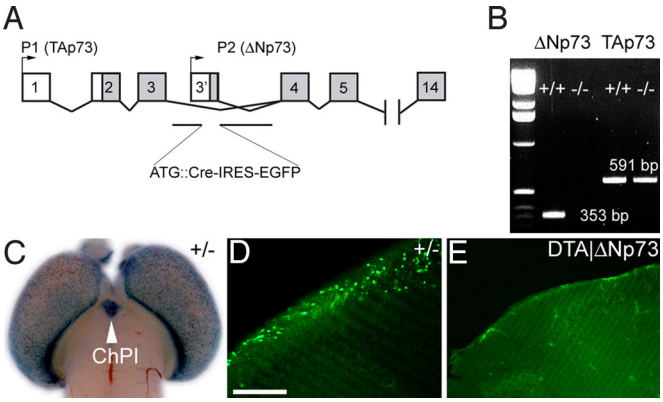


Fig. 1. Generation and validation of *DeltaNp73* mutant mice. (*A*) Genomic organization of the *p73* locus showing the two promoters that drive transcription of *TAp73* and *DeltaNp73*. A cassette encoding Cre and EGFP was inserted in frame with the start codon of *DeltaNp73* in exon 3′. (*B*) RT-PCR reactions on wild-type (+/+) and *DeltaNp73*$^{-/-}$ brain extracts at P0, using primers specific for *DeltaNp73* and TA*p73* isoforms. Note the normal amplification of *TAp73* (the 591-bp fragment) and absence of *DeltaNp73* transcripts in *DeltaNp73*$^{-/-}$ mutants (353 bp). (*C*) betaGal histochemistry on whole forebrain of a *LacZ*|*DeltaNp73* mouse at P0, showing labeled cells in the hemispheric marginal zone and choroid plexuses (ChPl, arrowhead). (*D*, *E*) Fluorescence microscopy at P0 detects EGFP signal from the knocked-in sequence in the marginal zone at P0 in *DeltaNp73*$^{+/-}$ mice (*D*) and absence of positive cells after genetic ablation in *DTA*|*DeltaNp73* mice (*E*).

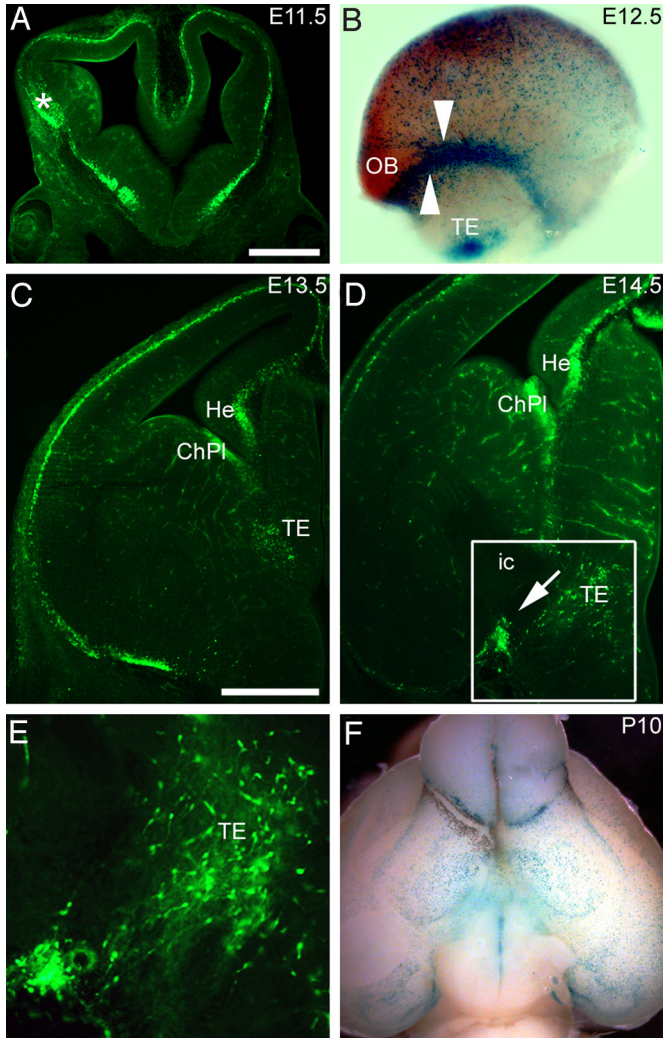


Fig. 2. Developmental expression of deltaNp73 in the forebrain, monitored by anti-GFP immunofluorescence (*A*, *C*, *D*, *E*) in *DeltaNp73*$^{+/-}$, and by βGal histochemistry (*B*, *F*) in *LacZ*| *DeltaNp73* mice. See text for detailed description. ChPl, chroid plexus; He, cortical hem; ic, internal capsule; OB, olfactory bulb; TE, thalamic eminence. Arrowheads point to the retrobulbar area. (*E*) is an enlargement of the TE, highlighted in another section in (*D*) with DeltaNp73 positive-neurons migrating from TE to ventral forebrain.

by using immunohistofluorescence with an anti-GFP antibody, as well as in double heterozygous mice obtained by crossing *DeltaNp73* mutant males with ROSA26R and ROSA-YFP reporter females (LacZ|DeltaNp73 and YFP|DeltaNp73). Results obtained with all approaches were consistent and confirmed previous studies with *in situ* hybridization (2, 16). At E11.5 and E12.5, a prominent population of DeltaNp73-positive cells was found in a rostral area located around the insertion of the olfactory bulb, the retrobulbar area (Fig. 2 *A* and *B*, arrowheads). From this position, cells appeared to migrate in the dorsal and ventral–basal cortical marginal zone (Fig. 2 *B–D*). A second focus of DeltaNp73 positive cells was the cortical hem, from where positive cells also spread in the marginal zone, primarily in medial cortical regions (Fig. 2 *C* and *D* and Fig. 3 *A–D*). A third zone was seen at the junction between presumptive pyriform and neocortices (Fig. 2*A* and Fig. 3*A*). At E13.5 and E14.5, these cells surrounded axons of the lateral olfactory tract. A fourth contingent of DeltaNp73-positive cells appeared at E11.5–E12.5 in a ventral region of the embryonic diencephalon, at the border between ventral diencephalon and telencephalon (Fig. 2*B*). Fluorescent neurons from this region formed a stream directed toward the ventral forebrain (Fig. 2 *D* and *E*, Fig. 3 *C* and *D*). The number of fluorescent cells decreased progressively with development, and no DeltaNp73 positive cell was found after birth. This area was also positive for calretinin and Tbr1 (Fig. S1), showing that it corresponds to the thalamic eminence (TE) (17). A fifth positive population was detected in preoptic area (Fig. 3 *K* and *L*). Previous studies of *p73* gene expression referred to a p73-positive region in the basal forebrain as the bed nucleus of stria terminalis (2). However, because there is no specific marker for this neuronal population and because p73 positive cells were found in rostral diencephalon, we prefer to refer to this zone as preoptic areas (POA). At P10, a few positive cells persisted in the cortical marginal zone, olfactory bulbs, and olfactory tubercles (Fig. 2*F* and Fig. S2 *E* and *F*). *p73*$^{-/-}$ mutant mice display prominent hydrocephalus (8, 18). To assess whether DeltaNp73 could be involved in cerebrospinal fluid (CSF) dynamics, we examined its expression in the ependyma and choroid plexuses. Although no expression was found in ependymal cells, choroid plexuses were heavily DeltaNp73 positive during embryonic development (Fig. 1*C*, Fig. 2 *C* and *D*, Fig. 3 *A–F*) and at postnatal stages (Fig. S3 *A* and *B*). They were reduced in size in *DeltaNp73*$^{-/-}$ animals, indicating that some of their epithelial cells died (compare Fig. 3*F* with 3*E*). In *DTA*|*DeltaNp73* mice, choroid plexuses were reduced to a few loops enriched in blood vessels. Yet, these animals looked unremarkable and exhibited neither hydrocephalus nor ventricle collapse (compare Fig. S3 *C* and *E* with Fig. S3 *D* and *F*), indicating that hydrocephalus in *p73*$^{-/-}$ mice may be *a vacuo* rather than related to defective CSF dynamics.

DeltaNp73 Is Required for Neuronal Survival. Numerous *in vitro* studies showed that DeltaNp73 promotes cell survival (6–11). The number of DeltaNp73-positive cells in the marginal zone, TE, and choroid plexuses was similar in heterozygous and homozygous *DeltaNp73* mutant mice at early developmental stages (Fig. S2 *A* and *B*). However, from E12.5, the number of labeled cells decreased progressively in *DeltaNp73*$^{-/-}$ as compared with heterozygous animals (compare Fig. 3 *B* and *D* with Fig. 3 *A* and *C*). Differences became obvious after birth (Fig. 3 *E–J* and Fig. S2 *E* and *F*). At P0, the number of Reelin-positive cells was reduced by half in

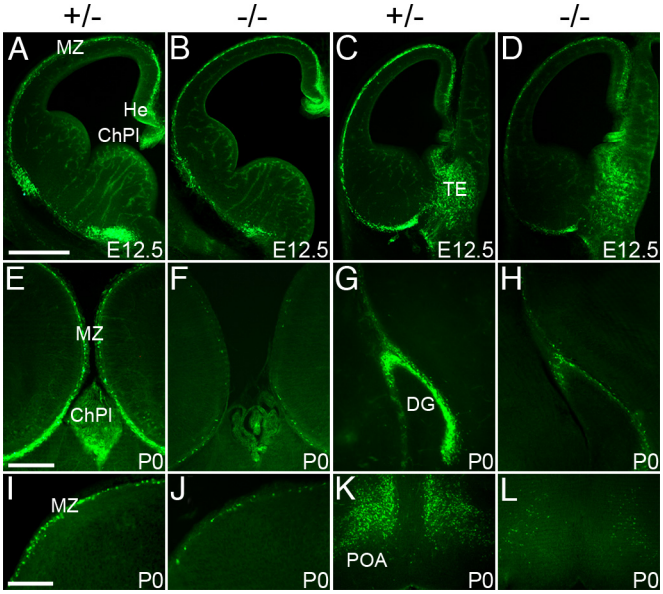


Fig. 3. DeltaNp73 promotes cell survival. (*A–D*) Anti-GFP immunofluorescence at E12.5 in *DeltaNp73* heterozygous (*A, C*) and homozygous (*B, D*) mice. A mild decrease in the number of DeltaNp73-positive cells is first perceived at that stage. (*E–L*) Fluorescence from knocked-in EGFP at P0 in *DeltaNp73* heterogygous (*E, G, I, K*) and *DeltaNp73* homozygous (*F, H, J, L*) mice. Cell death in homozygotes is evident in all DeltaNp73 expressing cell populations. He, cortical hem; TE, thalamic eminence; POA, preoptic area; ChPl, choroid plexuses (third ventricle); DG, dentate gyrus; MZ, cortical marginal zone.

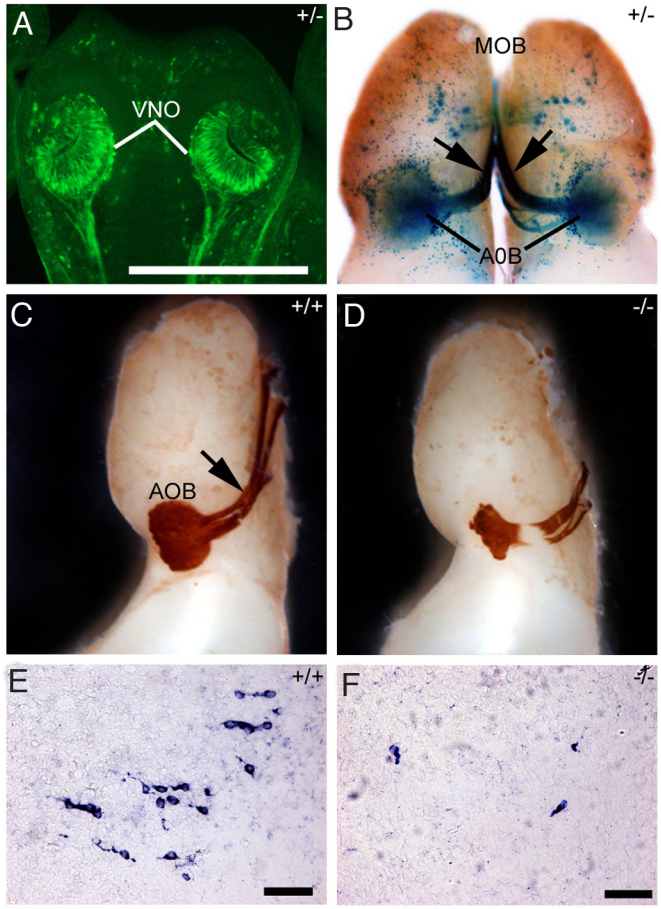


Fig. 4. DeltaNp73 mutation leads to reduction of the vomeronasal axons and GnRH neurons. (*A, B*) Expression of *DeltaNp73* in the VNO at E13.5 (*A*, GFP immunoflurescence), and in VNO axons (arrows) and their endings in the accessory olfactory bulbs (AOB) at P10 (*B*, βGal histochemistry). (*C, D*) SBA-HRP staining of VNO axons (arrow) in wild-type (*C*) and *DeltaNp73*$^{-/-}$ mutant adult mice (*D*). (*E, F*) *In situ* hybridization shows reduced number of GnRH positive cells in preoptic area of hypothalamus in *DeltaNp73*$^{-/-}$ (*F*) as compared with wild-type (*E*) mice. MOB, main olfactory bulbs.

DeltaNp73$^{-/-}$ mice (Fig. S2 *C* and *D*). These results indicate that DeltaNp73 promotes cell survival in living animals, as predicted from its activity in cell culture. However, CRc are a peculiar transient population, even in normal mice. To assess whether DeltaNp73 is also required for survival of other cells, we looked at other populations that express DeltaNp73, namely cells of the vomeronasal organ (VNO) and the preoptic area (2). Using endogenous EGFP expression, many DeltaNp73-positive cells were seen in the preoptic region of heterozygous animals at P0, but their number was reduced to almost nothing in *DeltaNp73*$^{-/-}$ homozygotes (Fig. 3 *K* and *L*). Strong DeltaNp73 related signal was demonstrated in a large subset of sensory neurons in the VNO, as well as in their axons and terminals in the accessory olfactory bulb (Fig. 4 *A* and *B*). In *DeltaNp73*$^{-/-}$ mice, VNO axons and terminals, visualized by staining with horseradish peroxidase (HRP)–coupled soybean agglutinin (19), were considerably reduced (Fig. 4 *C* and *D*). The time-limited fertility of *DeltaNp73* mutant mice and the abnormalities of the vomeronasal system prompted us to examine GnRH neurons. These neurons are generated in olfactory placodes and are believed to use vomeronasal axons to migrate to their final destination in the preoptic region and hypothalamus (20, 21). As shown in Fig. 4 *E* and *F*, the number of GnRH positive neurons, detected at P0 using *in situ* hybridization, was dramatically diminished in *DeltaNp73*$^{-/-}$ mutant, as compared with wild-type animals.

To understand better the effects of DeltaNp73 on neuronal survival, we assessed apoptosis by immunohistochemistry for activated caspase-3, at E13.5. Whereas no caspase-3–positive cells could be detected in CRc in WT mice, either in the cortical marginal zone or in the cortical hem, a few of these cells were clearly present in both locations in *DeltaNp73* homozygous mice (compare Fig. 5 *B* and *D* with Fig. 5 *A* and *C*). Those caspase-3–positive cells expressed GFP, confirming that DeltaNp73 deficient cells undergo apoptosis (Fig. S4). Moreover, in the trigeminal ganglion, where physiological apoptosis occurs, the number of caspase-3–positive profiles was drastically increased in mutant as compared with wild-type samples (Fig. 5 *E* and *F*). These observations show that *DeltaNp73* has antiapoptotic properties in vivo.

Genetic Ablation of CRc. Like Reelin, *p73* is heavily expressed in, and widely considered a marker of, CRc in various species (2, 22–24). To estimate the percentage of CRc that express DeltaNp73, we produced *LacZ|DeltaNp73* mice by crossing *DeltaNp73-Cre* male mice with *ROSA26R* females, and compared the number of cells positive for betaGal and Reelin in the cortical marginal zone at P0 (Fig. 6*A*). In all, 98% (317/325) of betaGal positive cells were also positive for Reelin, indicating that *DeltaNp73* expression is largely restricted to Reelin-positive neurons. On the other hand, 73% (317/433) of Reelin-positive cells were betaGal positive, showing that about one in four CRc never express DeltaNp73 during their development. The number of CRc positive both for Reelin and betaGal increased in gradient from the medial to the lateral and basal cortical fields. To genetically ablate CRc expressing DeltaNp73, we crossed *DeltaNp73-Cre* with *ROSA-DTA* mice to generate *DTA|DeltaNp73* animals. GFP visualization and Reelin immunohistochemistry in *DTA|DeltaNp73* mice showed that all EGFP-DeltaNp73–positive cells were removed (Fig. 1*E*), and that the number of Reelin-positive CRc was substantially reduced in marginal zones (Fig. 6*D*). A large contingent of CRc that are generated in the cortical hem and spread in the medial and lateral

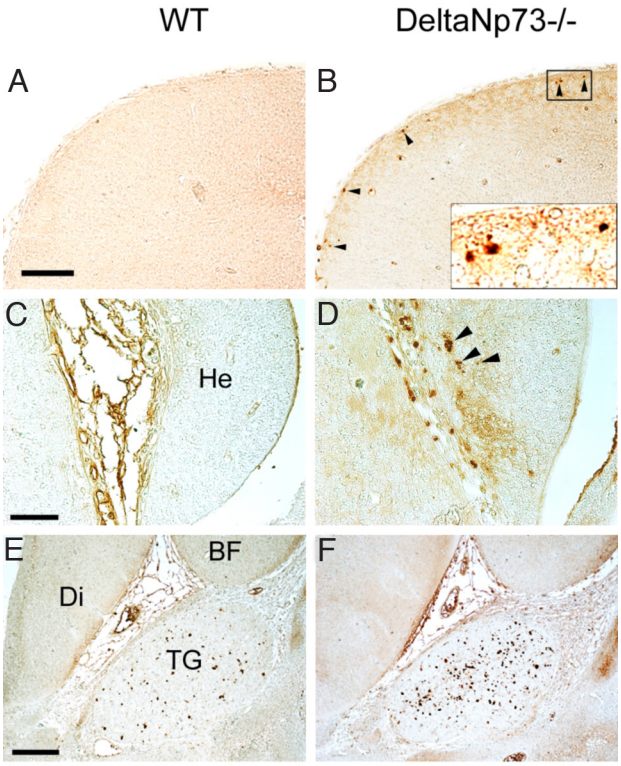


Fig. 5. DeltaNp73 deficiency leads to increased apoptosis. (*A–F*) Caspase-3 immunohistochemistry at E13.5 in cortical marginal zone (*A*, *B*). *Inset* in (*B*) is an enlargement of the squared region; cortical hem (*C*, *D*); and trigeminal ganglion (*E*, *F*). More Caspase3-positive cells were found in the mutant (*B*, *D*, *F*) as compared with littermate embryos (*A*, *C*, *E*). BF, basal forebrain; Di, diencephalon; He, cortical hem; TG, trigeminal ganglion. Bar, 100 μm (*A*, *B*), 50 μm (*C*, *D*), and 200 μm (*E*, *F*).

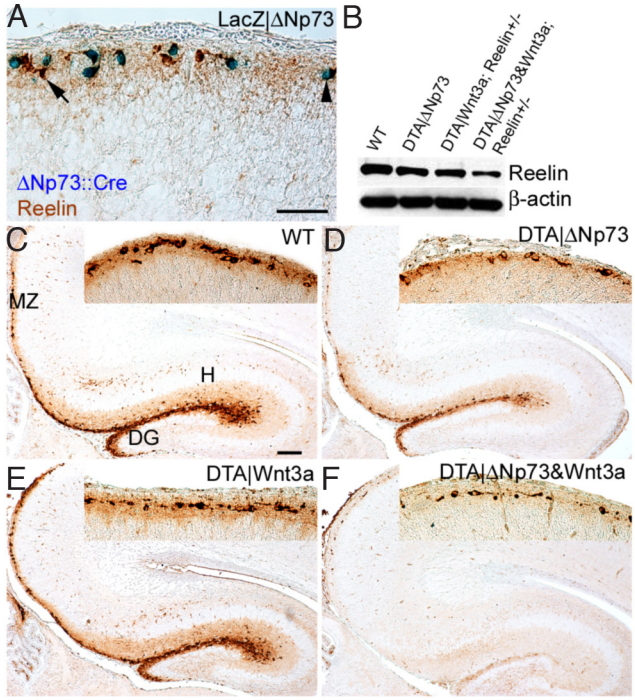


Fig. 6. DeltaNp73 is expressed in a large proportion of Reelin-positive CRc. (*A*) Colocalization of DeltaNp73 (βGal histochemistry, blue) and Reelin (immunohistochemistry, brown) in the cortical marginal zone at P0 in *LacZ|DeltaNp73* mice. Arrowhead shows CRc expressing both Reelin and DeltaNp73; arrow points to CRc that expresses only Reelin. (*B*) Western blot analysis of dorsal telencephalic extracts at E13.5. In contrast to the β-actin signal, which is similar in all genotypes, the Reelin signal decreases progressively when CRc are genetically ablated using *DeltaNp73-Cre*, *Wnt3a-Cre* and both. (*C–F*) Reelin immunohistochemistry of coronal sections at P0 confirms the appropriate decrease of Reelin-positive CRc from wild-type level (*C*) in *DTA|DeltaNp73* (*D*), *DTA|Wnt3a* (*E*), and *DTA|DeltaNp73&Wnt3a* mice (*F*). Note the complete loss of hippocampal CRc in the latter (*F*). *Insets* show enlargement of cortical marginal zone (MZ). DG, dentate gyrus; H, hippocampus.

cortical marginal zone derive from Wnt3a-positive precursors (16). To reduce further the number of CRc and the production of Reelin, we generated mice that bear combinations of the four alleles *DeltaNp73-Cre*, *Wnt3a-Cre*, *DTA*, and *reeler*. In these mice, CRc deriving from *DeltaNp73* and *Wnt3a* precursors express Cre and should be genetically ablated, and Reelin production in persisting Reelin-positive cells is reduced by half. In all genotypes, the architectonics of the cerebral cortical plate was unremarkable, unlike that in *reeler* mutant mice (Fig. S5). To estimate the relative concentrations of Reelin in the dorsal telencephalon, we carried out Western blot analyses of extracts from various genotype combinations at E13.5, the early cortical plate stage (Fig. 6*B*). Although the actin signal was similar in all samples, the Reelin signal was progressively decreased in *DTA| DeltaNp73* (Fig. 6*B*, *lane 2*), *DTA|Wnt3a & Reelin*$^{+/-}$ (*lane 3*), and in *DTA|Wnt3a&DeltaNp73 & Reelin*$^{+/-}$ (*lane 4*), as compared with the wild type (*lane 1*). However, the Reelin signal was consistently detected, even in quadruple heterozygotes. We then estimated the number of Reelin-positive cells in the cortical marginal zone using Reelin immunohistochemistry. Compared with wild-type brains (Fig. 6*C*), the number of CRc was reduced by 35% in *DTA|Wnt3a* (Fig. 6*E*), by 72% in *DTA|DeltaNp73* (Fig. 6*D*), and by 84% in *DTA|Wnt3a&DeltaNp73* (Fig. 6*F*). To further validate the activity of DTA, we performed double *in situ* hybridization for *Reelin* and *p73* and found that 210/279 (75%) of Reelin-positive cells coexpressed p73, which is consistent with the proportion of CRc ablated in *DTA|DeltaNp73* mice (Fig. S6). Because of the high density of Reelin-positive cells in the hippocampal formation, we found it impossible to count the number of cells that escaped genetic ablation in *DTA|Wnt3a* and *DTA|DeltaNp73* mice. In *DTA|Wnt3a&DeltaNp73* animals, however, almost all CRc were ablated from that region (Fig. 6*F*).

Discussion

In this work, we selectively inactivated the DeltaNp73 isoforms by inserting a cassette encoding the recombinase Cre along with EGFP. Using these reporters, we refine the expression pattern of p73 during development, identify the thalamic eminence (TE) as a contributor of neurons to the ventral forebrain, and confirm the multiple sources of CRc. When compared with wild-type littermates, homozygous *DeltaNp73* mutant mice display increased cell death in all p73 expressing cells. The number of CRc, POA, GnRH and VNO neurons is markedly reduced, and choroid plexuses are atrophic, yet the lamination of the cerebral cortex is normal. Genetic ablation of *DeltaNp73* positive cells severely damages choroid plexuses, but does not affect survival or result in any overt neurological phenotype.

DeltaNp73, a Marker of the Thalamic Eminence. A large number of strongly *DeltaNp73* positive cells are found in the ventral diencephalon at E11.5–E13.5. Contrary to CRc, these cells do not co-express Reelin, which is also detected in the diencephalon but at a more dorsal location, in presumptive reticular nuclei, including future zona incerta (25). Although the identity of these ventral diencephalic *DeltaNp73*-positive cells remains poorly defined, our observation that their number decreases rapidly while streams of cells with similar features are directed to the ventral telencephalon,

suggests strongly that they migrate and contribute to these areas rather than degenerating locally. The diencephalic *DeltaNp73*-positive region is also labeled with calretinin and Tbr1 antibodies and thus corresponds to the TE (17). That view receives support from comparative embryological observations. The TE is prominent in amphibians (26), and strongly *DeltaNp73*-positive cells are present in the embryonic reptilian ventral diencephalon (23). It is tempting to propose that the TE corresponds to the transient diencephalic perireticular nuclei (27), and that TE-derived cells might function as guidepost cells for axonal tracts in the internal capsule, such as the thalamocortical tract. Some support for that view is provided by the observation that thalamocortical connections fail to develop in *Celsr3|Dlx5/6* mice, in which Celsr3 is inactivated in a wide zone that encompasses the TE (28). Recently, a stream of Dbx1-positive cells, referred to as POA, was shown to originate in a diencephalic zone and to migrate to the amygdala (29). This diencephalic region is strongly reminiscent of the TE described here, including in its contributing neurons to the ventral forebrain. Neuronal migration from diencephalon to telencephalon is not widely investigated, and our *DeltaNp73* mutant mouse provides a useful tool for further studies of the TE and its contribution during development.

The *p73* Gene Family in Cell Death and Survival. The first genetic evidence for the involvement of p53 gene family in apoptosis came from the observation that approximately 25% of $p53^{-/-}$ females die *in utero* of exencephaly because of reduced cell death (30). This phenotype is reminiscent of that observed in mutants of Apaf-1, caspase 3, and caspase 9, all members of the mitochondrial cell death pathway. In $p73^{-/-}$ knock-out mice, in which all p73 isoforms are inactivated, the number of neurons of the superior cervical ganglion (SCG) is reduced by half (2, 7). In cultured SCG neurons, NGF removal results in neuronal death and decreased levels of DeltaNp73 proteins. Moreover, DeltaNp73 over expression rescues SCG neurons from NGF withdrawal induced apoptosis, and thwarts the effects of p53 overexpression, indicating that DeltaNp73 has prosurvival properties in SCG neurons, and that these properties are exerted, at least partially, by balancing the proapototic activity of p53 (7). Our in vivo study fully supports the role of DeltaNp73 in neuronal survival.

In $p73^{-/-}$ mice, the neural phenotype is much more severe than that observed in *TAp73* and *DeltaNp73* mutant mice. The massive loss of cortical neurons, hydrocephalus, and shortened lifespan described in $p73^{-/-}$ mice (8, 12) are found neither in *TAp73* (14, 31) nor in *DeltaNp73* $^{-/-}$ mice (this work). Usually, such differences are attributed to redundancy between closely related genes. However, many studies in cell culture have shown that TAp73 and DeltaNp73 have opposing rather than redundant effects on cell survival. Perhaps TAp73 and DeltaNp73, in addition to their reported opposing roles, may also act redundantly, and alterations in gene dosage may have an impact on the stoechiometry of complexes containing p73 as well as p53 and p63. Finally, the two known promoters that drive expression of TAp73 and DeltaNp73 may not be the only ones, and other, as yet uncharacterized alternative promoters may exist in the *p73* locus.

DeltaNp73 in the Vomeronasal System. The vomeronasal nerve is atrophic and the number of GnRH-positive hypothalamic neurons is drastically reduced in $DeltaNp73^{-/-}$ mice. These mice, particularly females, become prematurely infertile. The vomeronasal system is known to modulate sexual behavior and aggression, as well as pheromone responses (32). We did not observe any unusual sexual or aggressive behavior in $DeltaNp73^{-/-}$ mice. However, behavioral features related to VNO dysfunction require the complete removal of the system and the presence of residual vomeronasal neurons and terminals may thus prevent the appearance of behavioral traits in our mutant mice. On the other hand, vaginal plugs were observed in infertile females, indicating that the poor fertility in $DeltaNp73^{-/-}$ mice could be due either to endocrine dysfunction or to impaired pheromone perception by the VNO. A thorough endocrinological study of the hypothalamo-pituitary-gonadal axis would be needed to understand this better. Finally, it is worth noting that TAp63 and TAp73 play important roles in regulating the genomic stability of the female germ line during meiosis (31, 33), a feature that remains to be investigated in *DeltaNp73* mutants.

DeltaNp73, Reelin, and Cajal-Retzius Cells. CRc appear early in telencephalic marginal zones, and most disappear after birth in rodents (16, 34). They have multiple origins, notably in the medial ganglionic eminence, cortical hem, ventral pallium, and retrobulbar area, and migrate in subpial location by tangential routes (22, 35–39). Previous work showed that the loss of CRc cells in $p73^{-/-}$ mice (2) and in *Wnt3a-DTA|Emx1* hem-ablated mice (16), is compatible with normal neuronal layering of the cerebral cortex, unlike in Reelin-deficient (*reeler*) mice. These findings indicate that Reelin production is redundant during murine brain development and that death of most CRc is not sufficient to remove it completely.

Using Cre-mediated genetic ablation, we find that 35%, and 72% of Reelin positive are removed in *DTA|Wnt3a*, *and DTA|DeltaNp73* respectively. Furthermore, we show that Reelin is still detectable in the E13.5 dorsal telencephalon of embryos in which both Wnt3a and DeltaNp73 positive CRc have been genetically ablated, and Reelin gene dosage was further reduced by half. We failed to remove more CRc than in *Wnt3a-DTA|Emx1* mice in which very few CRc seemed to escape ablation in dorsal telencephalon, although no quantification was performed in that study (16). One possible explanation for this apparent discrepancy could be that *Wnt3a-Cre* may be less efficient than *Wnt3a-DTA*, so that some Wnt3a-positive cells escaped genetic ablation in our crosses.

We find that 70–75% of Reelin-positive CRc co-express p73, a proportion similar to that ablated in *DTA|DeltaNp73* mice, showing that our DTA allele is effective. In *DTA|DeltaNp73&Wnt3a*, more than 80%, but not all, of CRc were removed, yet reelin was still detectable. We suggest that residual Reelin is secreted by DeltaNp73- and Wnt3a-negative cells. Dbx1 is another CRc marker the expression of which overlaps that of DeltaNp73, particularly in basal forebrain (29, 37); some Dbx1-positive CRc might be negative for DeltaNp73 and Wnt3a and might contribute to the 16% of Reelin-positive CRc that persist after genetic ablation and to residual reelin detected in Western blot. Another possible source of reelin are neurons migrating from the ganglionic eminence (38), in which Reelin mRNA and protein are detected from E12.5. There is evidence that, in the murine cortex, very low concentrations of Reelin, even when secreted ectopically, suffice to normalize the reeler phenotype (40), suggesting that residual Reelin is sufficient to allow normal development. A subsidiary question that stems from these findings is why murine CRc produce such high levels of apparently redundant and unnecessary Reelin. Thus far, however, this intriguing question has received no satisfactory answer (24).

Materials and Methods

Animals. All animal experiments were carried out in accordance with national and institutional animal ethical guidelines. In addition to the *DeltaNp73* mutant strain described below, the following mutant mice were used: Cre reporter mice ROSA26R (41) and ROSA26-eYFP (42), reeler (Orleans allele) (43), Wnt3a-Cre (16), and conditional DTA (15). To describe genotypes in conditional mutant mice, we use the short notation ''anyGene|cre''; for example, DTA| DeltaNp73 stands for mice that are heterozygotes for DTA and Cre driven by DeltaNp73, in which DTA is activated conditional to DeltaNp73 expression (28).

Targeting of *DeltaNp73*. *DeltaNp73* mutant mice were generated by conventional gene-targeting procedures. The targeting construct contained a Cre-IRES-EGFP cassette inserted downstream from the 5′ homology region (Mm4_39308_37; nucleotides 7931161–7933301), which ends with the ATG codon of exon 3′, a Neo selection cassette flanked with FRT sites, the 3′ homology region (Mm4_39308_37; nucleotides 7920072–7923789), and a DTA negative selection

cassette. The construct was electroporated into R1 ES cells to isolate heterozygous ES cells. Injected B6 blastocysts were transferred to pseudopregnant CD1 female mice, and a colony was generated from chimeric animals and maintained by intercrosses. For further information see *SI Materials and Methods*.

RT-PCR. Total RNA was extracted using NucleoSpin RNA II kit (Macherey-Nagel). Contaminating genomic DNA was removed by treatment with DNase (Macherey-Nagel). RNA was converted to single-stranded cDNA using the ImProm-II reverse transcriptase (Promega) with random primer (0.5 μg/ml) in 20 μl of 1X ImProm-II buffer containing 6 mM MgCl2, 0.5 mM each dNTP, and 20U recombinant RNasin ribonuclease inhibitor. For subsequent PCR amplification, cDNA samples were incubated with 500 nM of each of the sense and antisense primers and 1 unit of recombinant Go Taq polymerase (Promega) in 20 μl of 1X PCR buffer. For further information see *SI Materials and Methods*.

Histology. Animals were deeply anesthetized before sacrifice. Postnatal mice were fixed by transcardial perfusion with paraformaldehyde (PFA, 4% in PBS) and embryos by immersion in PFA or Bouin's fluid. Samples were embedded in paraffin or cryoprotected for preparation of paraffin or cryostat sections, respectively. For histological studies, we used hematoxylin-eosin and Nissl staining on paraffin sections. For beta-galactosidase staining, whole brains or 100-μm thick vibratome sections were briefly fixed in 2% PFA; 0.1% glutaraldhehyde, and stained in 1 mg/ml Xgal, 5 mM K_3Fe (CN), 5 mM K_4F $(CN)_6$, and 2 mM $MgCl_2$ in PBS. For immunohistochemistry, the primary antibodies used were: chicken anti-GFP (1:1000, Aves Labs), mouse anti-Reelin (1:1000, G10) (44), rabbit anti-cleaved caspase-3 (1:200, Cell Signaling), rabbit anti-Tbr1 (1:2500, Chemicon), and rabbit anti-calretinin (1:2000, Swant). Signals were detected either by the ABC kit (Vector Labs) and DAB staining, or by immunofluorescence using the following secondary antibodies: goat anti-chicken fluorescein-conjugated (1:500, Aves Labs), goat anti-mouse IgG Alexa Fluor 594 (1:800, Invitrogen), and goat anti-rabbit IgG Alexa Fluor 594 (1:800, Invitrogen). *In situ* hybridization was performed with a digoxigenin-labeled GnRH probe as described (20). Double *in situ* hybridization was carried out using a digoxigenin-labeled probe for Reelin, and [^{33}P]-labeled probe for p73. To stain axons of vomeronasal neurons, we used HRP-labeled soybean agglutinin (SBA-HRP) (45). Brains were dissected to expose the accessory olfactory bulbs and incubated in 3% NGS, 1% H_2O_2 in PBS for 1 h, stained in 15 μg/ml SBA-HRP (Sigma) for 1 h at room temperature, and signal was detected with DAB for 5 min. Fluorescent preparations were examined with a Zeiss axioskop microscope, photographed with an Eclipse system (Nikon), and montages were edited with Photoshop (Adobe).

Western Blotting. Protein extracts were prepared from dorsal telencephalon of E13.5 embryos of different genotypes. Samples containing 10 μg proteins were fractionated by sodium dodecyl sulfate–polyacrylamide gel electrophoresis (SDS-PAGE), followed by transfer to nitrocellulose membranes. Reelin was detected using the G10 antibody (44), and the anti-beta actin antibody (Sigma) was used as loading control.

ACKNOWLEDGMENTS. We thank Elisabeth Grove for critical reading of the manuscript and for providing the Wnt3a-Cre mice; Philippe Soriano for the gift of several plasmids and cassettes used in the targeting; Nicoletta Kessaris for help with ROSA26R reporter mice; and Valérie Bonte, Isabelle Lambermont, and Esther Paitre for technical assistance. This work was supported by the grants from Actions de recherches concertées (ARC-186), FRFC 2.4504.01, FRSM 3.4501.07, Interuniversity Poles of Attraction (SSTC, PAI p6/20), Fondation médicale Reine Elisabeth, and from the Région Wallonne, all from Belgium. F.T. and A.R. are respectively research associate and postdoctoral researcher at the National Funds for Scientific Research (FNRS).

1. Kaghad M, et al. (1997) Monoallelically expressed gene related to p53 at 1p36, a region frequently deleted in neuroblastoma and other human cancers. *Cell* 90:809–819.
2. Yang A, et al. (2000) p73-Deficient mice have neurological, pheromonal and inflammatory defects but lack spontaneous tumours. *Nature* 404:99–103.
3. Yang A, Kaghad M, Caput D, McKeon F (2002) On the shoulders of giants: p63, p73 and the rise of p53. *Trends Genet* 18:90–95.
4. Flores ER, et al. (2005) Tumor predisposition in mice mutant for p63 and p73: Evidence for broader tumor suppressor functions for the p53 family. *Cancer Cell* 7:363–373.
5. Ramadan S, et al. (2005) p73 induces apoptosis by different mechanisms. *Biochem Biophys Res Commun* 331:713–717.
6. Simoes-Wust AP et al. (2005) DeltaNp73 antisense activates PUMA and induces apoptosis in neuroblastoma cells. *J Neurooncol* 72:29–34.
7. Pozniak CD, et al. (2000) An anti-apoptotic role for the p53 family member, p73, during developmental neuron death. *Science* 289:304–306.
8. Pozniak CD, et al. (2002) p73 is required for survival and maintenance of CNS neurons. *J Neurosci* 22:9800–9809.
9. Jacobs WB, Kaplan DR, Miller FD (2006) The p53 family in nervous system development and disease. *J Neurochem* 97:1571–1584.
10. Stiewe T, Putzer BM (2001) p73 in apoptosis. *Apoptosis* 6:447–452.
11. Grob TJ, et al. (2001) Human delta Np73 regulates a dominant negative feedback loop for TAp73 and p53. *Cell Death Differ* 8:1213–1223.
12. Meyer G, et al. (2004) Developmental roles of p73 in Cajal-Retzius cells and cortical patterning. *J Neurosci* 24:9878–9887.
13. Tomasini R, et al. (2008) TAp73 knockout shows genomic instability with infertility and tumor suppressor functions. *Genes Dev* 22:2677–2691.
14. Tomasini R, et al. (2009) TAp73 regulates the spindle assembly checkpoint by modulating BubR1 activity. *Proc Natl Acad Sci USA* 106:797–802.
15. Brockschnieder D, Pechmann Y, Sonnenberg-Riethmacher E, Riethmacher D (2006) An improved mouse line for Cre-induced cell ablation due to diphtheria toxin A, expressed from the Rosa26 locus. *Genesis* 44:322–327.
16. Yoshida M, Assimacopoulos S, Jones KR, Grove EA (2006) Massive loss of Cajal-Retzius cells does not disrupt neocortical layer order. *Development* 133:537–545.
17. Abbott LC, Jacobowitz DM (1999) Developmental expression of calretinin-immunoreactivity in the thalamic eminence of the fetal mouse. *Int J Dev Neurosci* 17:331–345.
18. Cabrera-Socorro A, et al. (2006) Multiple isoforms of the tumor protein p73 are expressed in the adult human telencephalon and choroid plexus and present in the cerebrospinal fluid. *Eur J Neurosci* 23:2109–2118.
19. Pankevich DE, Baum MJ, Cherry JA (2004) Olfactory sex discrimination persists, whereas the preference for urinary odorants from estrous females disappears in male mice after vomeronasal organ removal. *J Neurosci* 24:9451–9457.
20. Schwarting GA, Henion TR, Nugent JD, Caplan B, Tobet S (2006) Stromal cell-derived factor-1 (chemokine C-X-C motif ligand 12) and chemokine C-X-C motif receptor 4 are required for migration of gonadotropin-releasing hormone neurons to the forebrain. *J Neurosci* 26:6834–6840.
21. Cariboni A, et al. (2005) Reelin provides an inhibitory signal in the migration of gonadotropin-releasing hormone neurons. *Development* 132:4709–4718.
22. Meyer G, Perez-Garcia CG, Abraham H, Caput D (2002) Expression of p73 and Reelin in the developing human cortex. *J Neurosci* 22:4973–4986.
23. Cabrera-Socorro A, Hernandez-Acosta NC, Gonzalez-Gomez M, Meyer G (2007) Comparative aspects of p73 and Reelin expression in Cajal-Retzius cells and the cortical hem in lizard, mouse and human. *Brain Res* 1132:59–70.
24. Tissir F, Goffinet AM (2007) Reelin, Cajal-Retzius cells and Cortical Evolution. *Evolution of Nervous Systems*, ed Kaas JH (Elsevier, Amsterdam), Vol 1, pp 89–97.
25. Schiffmann SN, Bernier B, Goffinet AM (1997) Reelin mRNA expression during mouse brain development. *Eur J Neurosci* 9:1055–1071.
26. Krug L, Wicht H, Northcutt RG (1993) Afferent and efferent connections of the thalamic eminence in the axolotl, *Ambystoma mexicanum. Neurosci Lett* 149:145–148.
27. Mitrofanis J, Baker GE (1993) Development of the thalamic reticular and perireticular nuclei in rats and their relationship to the course of growing corticofugal and corticopetal axons. *J Comp Neurol* 338:575–587.
28. Zhou L, et al. (2008) Early forebrain wiring: Genetic dissection using conditional Celsr3 mutant mice. *Science* 320:946–949.
29. Hirata T, et al. (2009) Identification of distinct telencephalic progenitor pools for neuronal diversity in the amygdala. *Nat Neurosci* 12:141–149.
30. Armstrong JF, Kaufman MH, Harrison DJ, Clarke AR (1995) High-frequency developmental abnormalities in p53-deficient mice. *Curr Biol* 5:931–936.
31. Tomasini R, et al. (2008) TAp73 knockout shows genomic instability with infertility and tumor suppressor functions. *Genes Dev* 22:2677–2691.
32. Keverne EB (1999) The vomeronasal organ. *Science* 286:716–720.
33. Suh EK, et al. (2006) p63 protects the female germ line during meiotic arrest. *Nature* 444:624–628.
34. Frotscher M, Seress L, Abraham H, Heimrich B (2001) Early generated Cajal-Retzius cells have different functions in cortical development. *Symp Soc Exp Biol* 53:43–49.
35. Meyer G, Wahle P (1999) The paleocortical ventricle is the origin of reelin-expressing neurons in the marginal zone of the foetal human neocortex. *Eur J Neurosci* 11:3937–3944.
36. Takiguchi-Hayashi K, et al. (2004) Generation of reelin-positive marginal zone cells from the caudomedial wall of telencephalic vesicles. *J Neurosci* 24:2286–2295.
37. Bielle F, et al. (2005) Multiple origins of Cajal-Retzius cells at the borders of the developing pallium. *Nat Neurosci* 8:1002–1012.
38. Lavdas AA, Grigoriou M, Pachnis V, Parnavelas JG (1999) The medial ganglionic eminence gives rise to a population of early neurons in the developing cerebral cortex. *J Neurosci* 19:7881–7888.
39. Soda T, et al. (2003) Segregation and coactivation of developing neocortical layer 1 neurons. *J Neurosci* 23:6272–6279.
40. Magdaleno S, Keshvara L, Curran T (2002) Rescue of ataxia and preplate splitting by ectopic expression of Reelin in reeler mice. *Neuron* 33:573–586.
41. Soriano P (1999) Generalized lacZ expression with the ROSA26 Cre reporter strain. *Nat Genet* 21:70–71.
42. Srinivas S, et al. (2001) Cre reporter strains produced by targeted insertion of EYFP and ECFP into the ROSA26 locus. *BMC Dev Biol* 1:4.
43. Lambert de Rouvroit C, Goffinet AM (1998) The reeler mouse as a model of brain development. *Adv Anat Embryol Cell Biol* 150:1–106.
44. de Bergeyck V, Naerhuyzen B, Goffinet AM, Lambert de Rouvroit C (1998) A panel of monoclonal antibodies against reelin, the extracellular matrix protein defective in reeler mutant mice. *J Neurosci Methods* 82:17–24.
45. Key B, Giorgi PP (1986) Soybean agglutinin binding to the olfactory systems of the rat and mouse. *Neurosci Lett* 69:131–136.